

# Impurity Investigations by Means of Li-Beam Induced Charge Exchange Spectroscopy on W7-AS

FIEDLER Stefan, BRANDENBURG Roland<sup>1</sup>, BALDZUHN Jürgen<sup>1</sup>,

McCORMICK Kent, AUMAYR Fritz<sup>1</sup>, SCHWEINZER Josef,

WINTER Hannspeter<sup>1</sup> and the W7-AS Team

*Max-Planck-Institut für Plasmaphysik, EURATOM Ass., D-85748 Garching, Germany*

*<sup>1</sup>Institut für Allgemeine Physik, TU-Wien, EURATOM JEA Ass., A-1040 Wien, Austria*

(Received: 30 September 1997/Accepted: 22 October 1997)

## Abstract

Knowledge of the impurity concentration and temperature in the core plasma gradient region as well as the SOL is a vital element on the road to documenting and understanding the physics of L- or H-mode transport and the transport barrier itself. To this end, the Li-beam diagnostic capabilities on W7-AS have been expanded to include the measurement of radial profiles of ion impurity density and temperature via charge-exchange-spectroscopy (Li-CXS).

After briefly discussing the method of Li-CXS this paper describes the experimental setup on W7-AS and presents first results. Measurements of  $C^{6+}$ ,  $C^{5+}$  and  $B^{5+}$  spectral lines prove the viability of Li-CXS. In the plasma edge region ( $r_{\text{eff}} > 8$  cm) a  $C^{6+}$  concentration of about 0.5% could be measured. Temperature values found for  $C^{6+}$  are similar to proton/deuterium temperatures.

The intensities of several LiI spectral lines ( $2p \rightarrow 2s$ ,  $3d \rightarrow 2p$ ,  $4s \rightarrow 2p$ ,  $4d \rightarrow 2p$ ) have been measured and are used to critically check the underlying cross section database employed within the collisional-excitation Li-beam model, especially for collision processes involving higher Li-states ( $n \geq 3$ ). It was found that the ratio of the  $3d \rightarrow 2p$  and  $2p \rightarrow 2s$  spectral lines is overestimated by the model but is within uncertainties in the cross section database.

## Keywords:

diagnostics, atomic beam, Lithium, charge exchange spectroscopy, impurity density, electron density, impurity temperature

## 1. Introduction

Li-beam diagnostics are a multi-purpose technique for investigating fusion edge plasmas. While the determination of electron densities by lithium impact excitation spectroscopy (Li-IXS) has already reached a satisfactory standard on both large fusion experiments at IPP Garching [1,2], neutral Li-beams can also be used to determine local concentrations as well as temperatures of impurity ions via charge exchange spectroscopy (Li-CXS) [3,4]. This method has been proposed by Winter [5] and was applied for the first time at the

TEXTOR tokamak at KFA Jülich [6,7]. In order to achieve simultaneous Li-IXS and Li-CXS measurements, the present setup for electron density measurements has been extended. First results prove the feasibility of Li-CXS with the improved Li-injector [1] in W7-AS plasmas.

## 2. Principles

From observation of the resonant line radiation profile from the injected Li-beam it is possible to deduce the

Corresponding author's e-mail: Stefan.Fiedler@ipp-garching.mpg.de

electron density profile as well as the local  $\text{Li}(nl)$  state distribution along the injected Li-beam by modeling the Li-beam-plasma interaction. In addition to the impact excitation process the weakly bound outer electron of the Li-atom can also be captured by impurity ions. This charge exchange process populates highly excited states of the impurity ions, giving subsequently rise to characteristic impurity line radiation. Observation of this line emission in conjunction with the calculated  $\text{Li}(nl)$  state distribution allows evaluation of the impurity density profile along the injected Li-beam. Finally the temperature profile of the impurity ions is determined from the spectral line shape.

### 3. Experimental Setup on W7-AS

The existing Li-beam diagnostic layout [1] has been supplemented by a 14 channel observation system with a radial resolution of  $\delta r \sim 6$  mm for a range of  $\sim 13$  cm along the beam, corresponding to an effective plasma radius from 3 to 17 cm, *cf.* Fig. 1. Two glass achromats ( $\Omega/4\pi \sim 2.9 \times 10^{-4}$  sr) image the light onto 14 bundles, each consisting of a  $2 \times 4$  array of  $400 \mu\text{m}$  quartz fibers. The bundles are coupled one by one to the entrance slit of a monochromator (ACTON, Czerny-Turner,  $f=0.75$  m) to permit spectral resolution for Li-CXS and LiI radiation. A two-dimensional detector (Proscan CCD camera,  $512 \times 512$  pixels, each

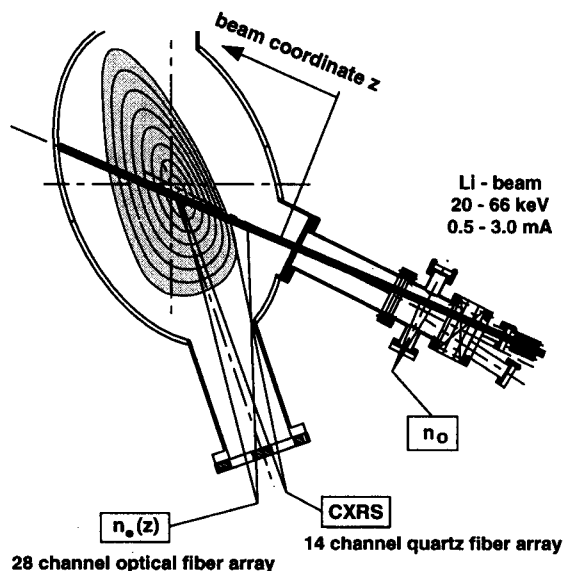


Fig. 1 Experimental set-up on the W7-AS stellarator. The observation geometry for Li-IXS (28 channels), Li-CXS (14 channels) and neutral density  $N_0$  is indicated.

$19 \times 19 \mu\text{m}^2$ ) is directly connected to the monochromator exit. The spectral resolution can reach up to  $0.018$  nm/pixel, using a  $1800$  g/mm holographic grating (blazing for  $500$  nm). An additional system of R928 or R3896 Hamamatsu photomultipliers in conjunction with interference filters ( $\lambda = 529.0$  nm for  $\text{C}^{6+}$ ,  $\delta\lambda_{1/2} \sim 5 \text{ \AA}$ ) can be coupled to the same light guides for simultaneous measurements at the 14 radial locations.

The extraction geometry of the Li-beam injector was changed to increase the Li-beam current delivered by the gun [1]. These experiments were carried out at  $50$  keV injection energy with a equivalent neutral Li-beam current of  $1.9$  mA and a Li-beam diameter of  $D_{\text{FWHM}} \leq 1$  cm.

### 4. Lithium Beam Composition

Since highly different cross sections for charge exchange processes follow from different excitation states of the donor atom, the composition of the Li-beam is of great importance for evaluating CXS data. We have therefore investigated several LiI spectral lines ( $2p \rightarrow 2s$ ,  $3d \rightarrow 2p$ ,  $4s \rightarrow 2p$ ,  $4d \rightarrow 2p$ ) in W7-AS discharges. While the measurements of the most relevant line  $\text{Li}(2p \rightarrow 2s)$  at  $\lambda = 670.8$  nm were performed to calibrate the CXS setup relative to the Li-IXS photomultiplier setup (see below), all other LiI lines were investigated to check the attenuation model of the Li-beam [8]. Measured intensities of emission from higher levels were found to differ considerably (30–60%) from corresponding theoretical values. We observed no dependence on magnetic field strength and beam energy (20–66 keV). The plasma density had a strong influence on the conformity of experimental and theoretical values, with the deviation becoming larger at higher densities.

As the major reason for these disagreements, inadequate scaling relations for excitation and ionization processes involving protons and impurity ions in the underlying database [9] have been identified. These are now being recalculated by more advanced means. However, since the relative population of the  $\text{Li}(3d)$  level in the Li-beam is in the range of 1% only, and populations of all other  $\text{Li}(nl)$  levels ( $n > 2$ ) are even smaller, the influences of cross section discrepancies on electron density calculations remain below 10%.

Furthermore, recent simulations have suggested that the population of higher excited states depends on  $Z_{\text{eff}}$ . Thus, the measurement of only one additional line besides the resonance line offers a possibility to determine an estimate for  $Z_{\text{eff}}$  under the assumptions that a reasonable radial charge state distribution of the impurities is given and that the present disagreement for

$n=3$  populations between simulation and experiment diminishes as a consequence of more accurate cross sections.

## 5. CXS Investigations

### 5.1 Impurity density profiles

To determine the absolute concentration of  $C^{6+}$  impurity ions, both Li-beam diagnostic systems are necessary (IXS and CXS). While the IXS system (28 PM) records the  $Li(2p)$  light emission, the CXS system (CCD-camera) delivers the CVI line radiation at 529.0 nm. Since both systems use different observation optics the detection efficiency has to be cross-calibrated. This is done by measuring the  $Li(2p)$  light with both systems, the IXS-PM- $(U_{2p}^{PM}(i))$  and the CXS-CCD-system  $(U_{2p}^{CCD}(i))$ , respectively in a calibration discharge.

$$U_{2p}^{PM}(i) = k_{671}^{PM}(i) \cdot n_{Li} \cdot A_{2p-2s} \cdot N(2p) \quad (1a/b)$$

$$U_{2p}^{CCD}(i) = k_{671}^{CCD}(i) \cdot n_{Li} \cdot A_{2p-2s} \cdot N(2p)$$

$k$  denotes the detection efficiency for the two systems at  $\lambda=671.0$  nm,  $i$  the corresponding radial channel,  $A_{2p-2s}$  the transmission probability,  $n_{Li}$  the particle density of the Li-beam and  $N(2p)$  the relative occupation number of the  $2p$ -state. The CXS-signal  $(U_{529}^{CCD}(i))$  can be expressed by

$$U_{529}^{CCD}(i) = k_{529}^{CCD}(i) \cdot v_{Li} \cdot n_{C^{6+}} \cdot n_{Li} \cdot \sum_{nl} \sigma_{529}(nl) \cdot N(nl). \quad (2)$$

Calculating the ratio of eqs. 1b and 2 for the discharges in question and using the ratio of eqs. 1a and 1b for the calibration discharge, the  $C^{6+}$  density can be expressed by

$$n_{C^{6+}}(z_{Li}(i)) = \frac{U_{529}^{CCD}(i)}{U_{2p}^{PM}(i)} \cdot \frac{k_{671}^{PM}(i)}{k_{671}^{CCD}(i)} \cdot \frac{k_{671}^{CCD}(i)}{k_{529}^{CCD}(i)} \cdot \frac{A_{2p-2s} \cdot N(2p)}{v_{Li} \cdot \sum_{nl} \sigma_{529}(nl) \cdot N(nl)}. \quad (3)$$

In Eq. 3 the first ratio describes the measured signal ratio (IXS and CXS systems), the second ratio is determined by the calibration procedure (see above) and the third ratio expresses the different detection probabilities of the CCD camera for the two wavelengths.  $v_{Li}$  denotes the Li-beam particle velocity and  $\sigma_{529}(nl)$  the cross section for charge exchange from the  $(nl)$ -level, giving rise to subsequent line radiation at  $\lambda=529.0$  nm.

The relative occupation numbers  $N(nl)$  of the Li-beam atoms are calculated in the reconstruction process for the electron density (Li-IXS). The described algorithm was applied in a series of equivalent discharges ( $P_{ECRH}=400$  kW,  $D_2$ ,  $\iota=0.34$ ,  $B_z=20.0$  mT, up/down limiters attached,  $\int n_e dl(\text{HCN})=2 \times 10^{19}$  m $^{-2}$ ) to determine the  $C^{6+}$  impurity ion density for different radial positions (different  $z_{Li}$  in eq. 3). The result is shown in Fig. 2. The  $C^{6+}$  impurity ion concentration increases from about 0.41% at  $r_{eff}=16.7$  cm to 0.63% at  $r_{eff}=8.3$  cm. In the gradient region of the profile good agreement is found with the result from the H-CXS diagnostic [10].

For a single light guide in the radial range of the maximum of the  $Li(2p)$  profile we also investigated the signal to background ratio for other impurity ions. While the ratio was about 0.25 for  $C^{6+}$  we found a ratio of 0.2 for  $C^{5+}$  and  $B^{5+}$  respectively, clearly demonstrating the applicability of Li-CXS also for these impurity ions. The exposure time of the CCD camera was about 5.7 ms with a readout time of 3 ms. Each 10 ms a CCD-picture was recorded. The Li-beam was chopped electronically with a beam on and off time of 40 ms each. Thus 4 CCD-pictures could be used to determine Li-CXS and background signals. For the determination of impurity densities the Li-CXS signals were summed over the Li-beam on-time interval (40 ms). No impurity ion concentrations giving rise to CXS-line radiation in the UV-spectral range could be investigated, due to insufficient transmission of the observation optic (glass).

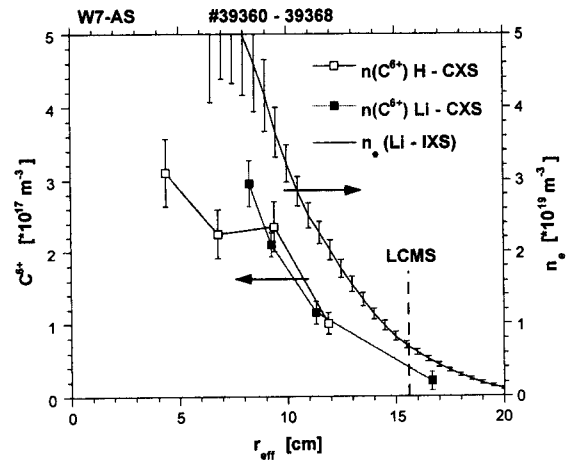


Fig. 2 Radial impurity density profile of  $C^{6+}$  and electron density profiles as a function of effective radius  $r_{eff}$  for discharges #39360-39368. The last closed magnetic surface (LCMS) is indicated by a dotted line.

## 5.2 Impurity temperature profiles

Temperature values are obtained by fitting a Gaussian profile to the CCD-camera data. To reduce the scatter of the calculated spectral line width, all CCD-pictures taken in the flat top phase of one discharge had to be summed. This typically implies a integration time of about 300–400 ms. The time resolution will be improved by a better coupling of the light guide bundles to the spectrometer entrance slit, where now an important fraction of the light signal is being lost.

For the fitting procedure line broadening effects such as Zeeman splitting and l-level mixing are taken into account [7].  $C^{6+}$  temperature values in the plasma edge obtained in the same series of discharges (see above) are shown in Fig. 3. For  $r_{\text{eff}} < 12$  cm  $C^{6+}$  temperature values are similar to proton/deuteron temperatures measured via active neutral particle analysis [11].

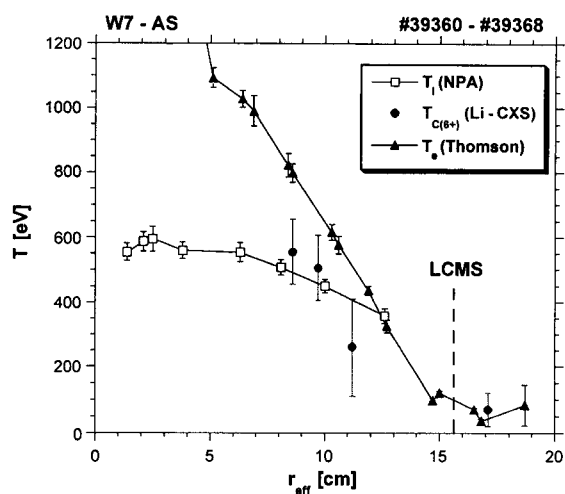


Fig. 3 Radial impurity temperature profiles of  $C^{6+}$ , electron temperature  $T_e$ , and deuterium temperature  $T_{D^+}$  measured by neutral particle analysis (NPA).

## 6. Conclusion

With the improved Li-injector now available we have demonstrated the applicability of Li-CXS, both for impurity density and impurity temperature measurements, on the W7-AS stellarator. Concentrations found for  $C^{6+}$  ions are in the order of 0.5%. The radial profile in the gradient region coincides with values from the  $H^0$ -CXS-diagnostic. Temperature values in the plasma edge can be considered to be equal to those for deuterium ions. Radial and temporal resolutions of 0.5 cm and 40 ms, respectively (400 ms for temperature measurements) could be achieved. By improving the detection efficiency, mainly by new fibers with smaller aperture and a new construction of the fibers-spectrometer coupling, the temporal resolution can probably be increased by more than a factor of 5.

## Acknowledgments

This work has been supported by Friedrich Schiedel-Stiftung für Energietechnik and by Kommission zur Koordination der Kernfusionsforschung at the Austrian Academy of Sciences.

## References

- [1] K. McCormick *et al.*, *Fusion Engineering and Design* **34-35**, 125 (1997).
- [2] S. Fiedler, IPP Report III/209 (1995).
- [3] E. Wolfrum *et al.*, *Rev. Sci. Instrum.* **64**, 2285 (1993).
- [4] F. Aumayr *et al.*, *J. Nucl. Materials* **196-198**, 928 (1992).
- [5] H. Winter, *Comments At. Mol. Phys.* **12**, 165 (1982).
- [6] R.P. Schorn *et al.*, *Appl. Phys. B* **52**, 71 (1991).
- [7] R.P. Schorn *et al.*, *Nucl. Fusion* **32**, 351 (1992).
- [8] J. Schweinzer *et al.*, *Plasma Phys. Control. Fusion* **34**, 1173 (1992).
- [9] D. Wutte *et al.*, *At. Nucl. Dat. Tables* **65**, 155 (1997).
- [10] J. Baldzuhn *et al.*, *Rev. Sci. Instrum.* **68**, 1020 (1997).
- [11] M. Kick *et al.*, *20th EPS Conf., Europhys. Conf. Abstr.* **17C Part I**, p.357 (1993).